Molecular characterization of a common fragile site (*FRA7H*) on human chromosome 7 by the cloning of a simian virus 40 integration site

DAN MISHMAR[*][†], AYELET RAHAT[*][†], STEPHEN W. SCHERER[‡], GERALD NYAKATURA[§], BERND HINZMANN[§], YOSHINORI KOHWI[¶], YAEL MANDEL-GUTFROIND[‖], JEFFREY R. LEE[‡], BERND DRESCHER[§], DEAN E. SAS[‡], HANAH MARGALIT[‖], MATTIAS PLATZER[§], ARYEH WEISS[*], LAP-CHEE TSUI[‡], ANDRÉ ROSENTHAL[§], AND BATSHEVA KEREM[*],[**]

[*]Department of Genetics, The Hebrew University, Jerusalem, Israel 91904; [‡]Department of Genetics, The Hospital for Sick Children, Toronto, ON M5G 1X8, Canada; [§]Department of Genome Analysis, The Institute for Molecular Biotechnology, Jena 07745, Germany; [¶]Lawrence Berkeley Laboratory, University of California, Berkeley, CA 94720; and [‖]Department of Genetics and Biotechnology, The Hebrew University, Hadassah, Jerusalem, Israel 91120

ABSTRACT   Common fragile sites are chromosomal loci prone to breakage and rearrangement, hypothesized to provide targets for foreign DNA integration. We cloned a simian virus 40 integration site and showed by fluorescent *in situ* hybridization analysis that the integration event had occurred within a common aphidicolin-induced fragile site on human chromosome 7, *FRA7H*. A region of 161 kb spanning *FRA7H* was defined and sequenced. Several regions with a potential unusual DNA structure, including high-flexibility, low-stability, and non-B-DNA-forming sequences were identified in this region. We performed a similar analysis on the published *FRA3B* sequence and the putative partial *FRA7G*, which also revealed an impressive cluster of regions with high flexibility and low stability. Thus, these unusual DNA characteristics are possibly intrinsic properties of common fragile sites that may affect their replication and condensation as well as organization, and may lead to fragility.

Fragile sites are specific chromosomal loci prone to breakage and characterized by constrictions, gaps, or breaks on chromosomes from cells exposed to specific tissue culture and chemical conditions (1). Fragile sites are classified as either rare or common, depending on their frequency within the population and their mode of induction. The instability of fragile sites at the molecular and cytogenetic levels can lead to disease manifestation by silencing adjacent gene(s) (2, 3) or by causing chromosomal rearrangements and disrupting gene expression (4). Several rare fragile sites have been characterized at the molecular level by positional cloning using families expressing these sites (4–9). The expression of these sites is associated with expanded CGG trinucleotide repeats or with an expanded 33-bp A+T-rich minisatellite repeats. The mechanism by which the repeat expansion is associated with the cytogenetic expression and chromosomal breakage of these sites is not well understood.

Common fragile sites ($n < 100$), on the other hand, are considered to be part of the normal chromosome structure. Most of these sites are induced by aphidicolin, an inhibitor of the elongation activity of DNA polymerases (10). Because common fragile sites are part of the normal chromosome, cloning of these sites could not use positional cloning approaches. Two strategies were described for the cloning of the fragile site at 3p14.2 (*FRA3B*). One was based on the observation that many chromosomal rearrangements and cancer

breakpoints fall within chromosomal bands to which fragile sites have been mapped. The second strategy was based on the hypothesis that fragile sites are recombinogenic and that foreign DNA might preferentially integrate into these sites. These studies led to the identification of *FRA3B,* which spans a region greater than 250 kb (11–17). More recently, several yeast artificial chromosome (YAC) clones were found to span a common aphidicolin-induced fragile site on human chromosome 7, *FRA7G* (18). However, the precise region of *FRA7G* is yet to be defined.

Partial sequences of *FRA3B* (276 kb) revealed no expanded repeats or other features that could clearly point to the molecular basis of its fragility (12–14, 16). Thus, additional common fragile sites had to be cloned and sequenced to enable the identification of characteristics shared by common fragile sites that are implicated in the instability of these sites.

Here we report the identification and characterization of a common aphidicolin-induced fragile site, *FRA7H*, on human chromosome 7. Our approach was based on previous cytogenetic observations linking viral integration sites and fragile sites (19, 20).

MATERIALS AND METHODS

Cell Lines. Two cell lines were used in this study: GM00847 (NIGMS, Camden, NJ), a simian virus 40 (SV40)-transformed human fibroblast cell line, and GM10791A (NIGMS), a chromosome 7 somatic cell hybrid.

Phage Genomic Library Construction. *Sau*3A partially digested DNA (9–23 kb), extracted from the cell line GM00847, was used to contract a λ-Dash-II library (Stratagene).

Genomic Libraries Used for Contig Constructions. A YAC library (21), a human P1-derived artificial chromosome (PAC) library (22), and a chromosome 7-specific cosmid library constructed from GM10791A were used.

Chromosome Preparation and Fragile Site Induction. Cells were grown on coverslips and fragile sites were induced by growing the cells in M-199 medium in the presence of 0.4 μM aphidicolin and 0.5% ethanol for 24 h prior to chromosome fixation using standard procedures.

Fluorescent *in Situ* Hybridization (FISH). Cosmid and YAC DNA were labeled with digoxigenin (DIG)-11-dUTP (Boehr-

---

Abbreviations: YAC, yeast artificial chromosome; SV40, simian virus 40; FISH, fluorescent *in situ* hybridization; EST, expressed sequence tag; MAR, matrix attachment region; CAA, chloroacetaldehyde.
Data deposition: The sequence reported in this paper has been deposited in the GenBank database (accession no. AF017104).
[†]D.M. and A.R. contributed equally to this work.
[**]To whom reprint requests should be addressed at: Department of Genetics, The Life Sciences Institute, The Hebrew University, Jerusalem, Israel 91904. e-mail: kerem@leonardo.ls.huji.ac.il.

inger Mannheim) by nick-translation. FISH was performed as previously described (23).

Analysis of Hybridization Signals. Green and red fluorescence signals were visualized simultaneously by using a Nikon B-2A filter cube. For weak signals a modified Chromatech HQ-FITC (Chroma Technology, Brattleboro, VT) filter set was used (excitation band, 460–500 nm; emission band, 520–600 nm). Images were captured with an intensified charge-coupled device imager (Paultek Imaging, Grass Valley, CA) and digitized with a frame grabber (Imascan/MONO-D, Imagraph, Chelmsford, MA).

Because there are several aphidicolin-induced fragile sites on 7q their positions had to be carefully determined. The Image-Pro PLUS program (Media Cybernetics, Silver Spring, MD) was used to measure the fragile site-telomere distance relative to the short arm length. According to the Genome Database (GDB 6.0), this value should be ≈45% for *FRA7H*, ≈82% for *FRA7G,* and ≈11% for *FRA7I*. Analysis based on 100 random measurements indicated that the standard deviation (SD) was 5%. Thus, observed cytogenetic gaps at fragile sites of 35–55% (two SD) were considered to be *FRA7H*.

Sequencing. Shotgun sequencing was performed as previously described (24).

Sequence Annotation. Computer analysis was performed by using our newly developed automated tool, RUMMAGE (B.D., J. Weber, R. Schattevoy, and A.R., unpublished work), which combines 23 different programs, including CENSOR, BLAST version 1.4, FASTA version 2.0, GRAIL, FEXHB, and MZEF. CpG islands were identified by using the following criteria: G+C > 50%, CpG ratio observed/expected >0.6, and length >200 bp. We also developed a tool, EXONSAMPLER, that filters and associates expressed sequence tag (EST) matches and verifies splice sites (J. Weber, B.D., and A.R., unpublished work). Repeat analysis was also performed, using REPEATER (R. Gill-More and M. Amitai, personal communication). The following programs from the Genetics Computer Group (GCG) were used: FINDPATTERNS, MAP, BESTFIT, GAP, COMPOSITION, FETCH, REPEAT, STEMLOOP, and SHUFFLE.

Computer Analysis of Helix Flexibility and Stability. The flexibility parameter that we used measured potential local variations in the DNA structure, expressed as fluctuations in the twist angle (25). The analysis was performed in overlapping windows of 100 bp. Dinucleotide values were summed along the window and averaged by the window length. Windows with outstanding values, deviating significantly from the average, were considered as potential flexible regions. Helix stability was based on the sequence-dependent free energy values of the helix-to-coil transition, and it is expressed in kcal/mol (1 kcal = 4.18 kJ) (26). The analysis was performed as described for DNA flexibility.

Identification of Potential Non-B-DNA Sequences. DNA sequences that potentially form a non-B-DNA structure under negative superhelical strain were manually scanned in the entire *FRA7H* region. We highlighted homopurine/homopyrimidine sequences of >30 nucleotides, other than poly(A) or poly(T), that readily form intramolecular triple-helix structures (27). We also searched for potential nuclear matrix attachment regions (MARs) by identifying relatively A+T-rich sequences (>70%) in which one strand consists exclusively of mixed As, Ts, and Cs, but not Gs (ATC sequences) (28). Only two stretches of ATC sequences, one of at least 18 nucleotides and the other of at least 16, separated by not more than 10 nucleotides were highlighted.

Non-B-DNA Structure Analysis. Non-B-DNA structures were detected by chloroacetaldehyde (CAA) *in vitro* (29). In brief, supercoiled plasmid DNA was reacted with 2 μl of double-distilled CAA in a 100-μl reaction volume at 37°C with or without 2 mM MgCl$_2$ at pH 7 (50 mM Tris·HCl). CAA-modified DNAs were end labeled with [^{32}P]dATP at the *Sal*I site (the 4.4-kb plasmid) or at the *Bam*HI site (the 2.2-kb plasmid) and further cleaved at a distal *Kpn*I site. DNA fragments were isolated and subjected to hydrazine and piperidine for the detection of mod-

ified adenines or formic acid and piperidine for the detection of modified cytosines. The cleavage products were resolved on a denaturing urea/polyacrylamide gel.

RESULTS AND DISCUSSION

Cloning of the SV40 Integration Site. We have studied an SV40-transformed human fibroblast cell line, GM00847, in which several viral genomes have integrated in 7q31–35 in tandem (30, 31). Because there are two common fragile sites in this region, *FRA7G* in 7q31.2 and *FRA7H* in 7q32.3, we speculated that the viral genomes might have integrated into one of these fragile sites. Therefore, as the first step toward cloning a common fragile site, a phage genomic library was constructed from the GM00847 cell line and screened for the SV40 integration site by using SV40 DNA as a probe. Four clones were identified, all sharing the same human-SV40 junction fragment.

Identification of *FRA7H* and Association with the SV40 Integration Site. A repeat-free 2.2-kb *Eco*RI fragment adjacent to the human-SV40 junction fragment was used to screen a YAC library. Nine unique clones were identified and used to construct a YAC contig of ≈8 Mb covering the entire 7q32 region (Fig. 1). These YAC clones were mapped to distinct cytogenetic bands in chromosome 7 by using FISH (32). The order of the clones and DNA markers was consistent with the radiation hybrid mapping from the Massachusetts Institute of Technology/Whitehead Genome Center and the genetic data from the Genethon linkage map.

To test if the SV40 integration site was at the same region as *FRA7H* and to clone the *FRA7H* genomic region, we performed FISH analysis using YAC clones containing the integration region as probes, on metaphase chromosomes induced to exhibit fragile sites (Fig. 2). The expression of fragile sites in the studied cell line (GM00847) is due to aphidicolin induction and is not observed in untreated cells. Four YAC clones harboring the SV40 integration site—HSC7E186, HSC7E555, HSC7E1029 (all three pink), and HSC7E430 (light blue) (Fig. 1 and Table 1)—appeared to "span" the *FRA7H* gap. Hence, on different chromosomes from the same preparation their hybridization signals appeared centromeric or telomeric to the *FRA7H* gap, or crossed the *FRA7H* gap ("on"). The distant centromeric YAC clones HSC7E1289 (orange) and HSC7E752 (purple) showed hybridization signals only centromeric to *FRA7H,* and the distant telomeric YAC HSC7E648 (light green) showed signals only telomeric to *FRA7H* (Fig. 1 and Table 1). Thus, these clones are located outside the fragile region. To exclude the possibility that the analyzed fragile site in the GM00847 cell line is caused by the integrated SV40 genomes, we performed FISH analysis on the somatic cell hybrid GM10791A, which contains one copy of normal chromosome 7, with no SV40 sequences. FISH analysis using HSC7E186 (pink) showed hybridization signals spanning the *FRA7H* site (Fig. 2*B*): 2 signals were on the site and 6 were centromeric and 10 telomeric to the site, providing evidence that the analyzed *FRA7H* site spans the same genomic region in the two cell lines. Because the YAC clones spanning *FRA7H* contain the SV40 integration site, our observations suggest that the SV40 integration event occurred within the *FRA7H* site, supporting the hypothesis that fragile sites in the human genome might represent target sites for viral integration. FISH results with additional YAC clones (HSC7E125/HSC7E587, HSC7E464, and HSC7E195) flanking the *FRA7H* region showed inconsistency with the physical map over a region of about 1.5 Mb (Table 1, discussed below).

To define the *FRA7H* region more precisely, FISH analysis on the GM00847 cell line was performed, using cosmid clones mapped to the YACs spanning *FRA7H* (Fig. 3). Six of these clones—141e11 (purple), 108f11/92h2 (dark green), 72c11 (gray), 137 g12 (pink), 159c12, (light blue), and 35c9 (brown)—

Table 1. FISH analysis of YAC hybridization signals on chromosomes expressing *FRA7H*

YAC clone HSC7E-	Color	No. of signals		
		Centromeric	On	Telomeric
1289	Orange	15	—	—
752	Purple	9	—	—
464	Dark green	15	7	—
195	Gray	7	6	6
1029/555/186	Pink	18	6	17
430	Light blue	11	—	2
125/587	Brown	20	—	—
648	Light green	—	7	9

Analysis of hybridization signals on metaphase chromosomes expressing *FRA7H* from cell line GM00847. The clones are ordered in accordance with the physical map, centromeric (top of the table) to telomeric (bottom). The results of clones covering the same genomic region were combined. The colors mark YAC clones in Fig. 1.

showed hybridization signals centromeric, telomeric, and crossing *FRA7H* (Fig. 2*C* and Table 2). FISH analysis with one of these cosmids, 137g12 (pink), was performed also on the somatic cell hybrid GM10791A, which is the cell line used for construction of the cosmid library. Again, the hybridization signals spanned *FRA7H*: one signal crossed the site, five were centromeric, and five were telomeric. This result further indicates that in both cell lines the analyzed fragile site is in the same genomic region, estimated to span ≈160 kb. However, clones 62f7 and 210c9 showed FISH results inconsistent with the physical map (Fig. 3 and Table 2; discussed below).

Sequence Analysis of the *FRA7H* Region. To identify features at the nucleotide level that might provide insight into the molecular basis of the fragility of the *FRA7H* region, we completely sequenced a contig of 4 cosmids spanning the *FRA7H* region (Fig. 3). The final sequence of 161,155 bp (GenBank accession no. AF017104) was extensively analyzed for repetitive elements and regions with coding potential (for details see http://genome.imb-jena.de). The analysis indicated that the region is A+T-rich (58%). It is composed of 13.1% short interspersed elements, 13.8% long interspersed elements, 5% long terminal repeats, and 0.7% DNA transposons. No CGG or any other expended repeats were revealed. Thus, the molecular basis for the fragility of *FRA7H* is probably different from that of the rare fragile sites and does not require expanded repeats. Similarly, *FRA3B* also seems to lack expanded repeats (12–14, 16).

Numerous exons were predicted in *FRA7H*, but none by more than two different programs. It is likely that these predictions are false positives. BLAST similarity searches revealed a number of EST clones, none of which predicted exons. Resequencing of many of these EST clones revealed no ORFs. Similarity searches identified areas with 88% similarity to the zinc finger protein ZNF131 and 74% to histone H4. However, detailed analysis revealed that both are pseudogenes. The *ZNF131* pseudogene most probably resulted from integration of a *ZNF131* transcript into which subsequently several transposable elements integrated. The observation that several integration events occurred in *FRA7H* might be associated with the chromosomal instability of the region. These observations suggest that the region is gene poor. We could not
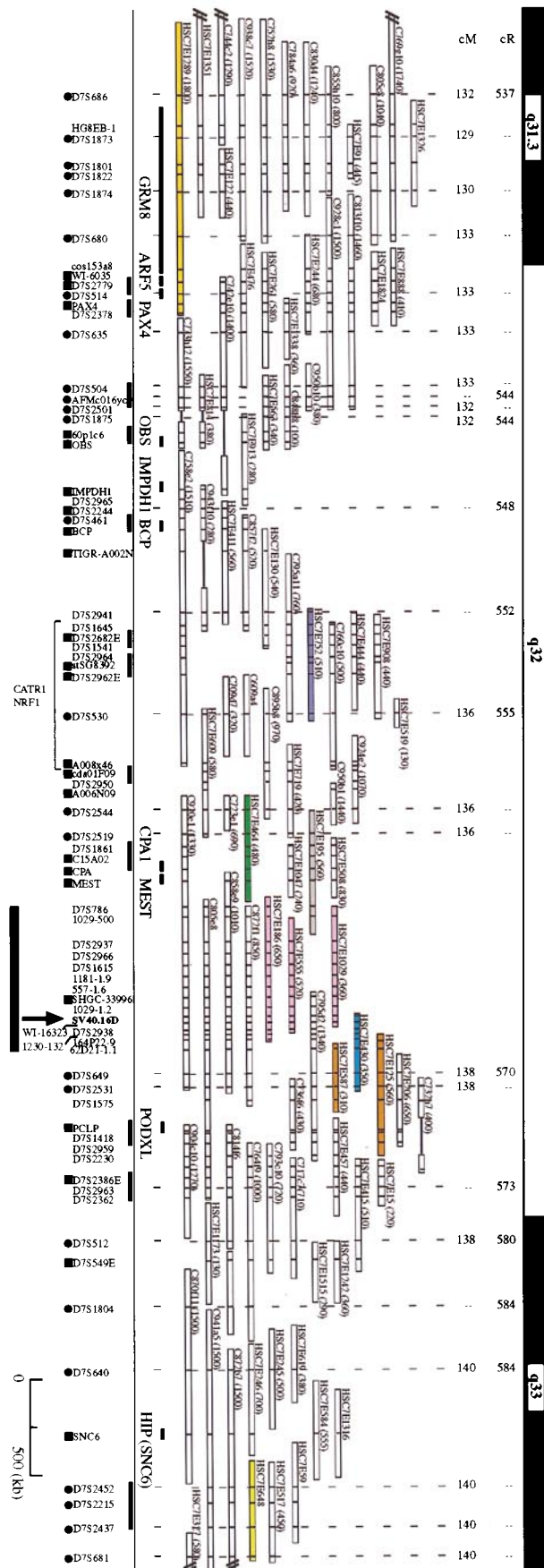
FIG. 1. A physical map across the 7q32 and *FRA7H* region. The order and extent of overlap of YAC clones was based on their DNA marker content. Distances from 7pter are shown in centirads (cR) and centimorgans (cM). Solid bar links DNA markers for which the local order could not be determined. ●, genetic markers; ■, ESTs/genes. Markers with no denotation are sequence-tagged sites (STSs) or unique DNA probes. Vertical bars within each YAC clone indicate the presence of a marker. YAC clones used for FISH analysis are colored. YAC clones that cover the same genomic region are marked by the same color. Solid box indicates the region shown in greater detail in Fig. 3. Information on this contig can be found in the Genome Database and at http://www.genet.sickkids.on.ca/chromosome7/.
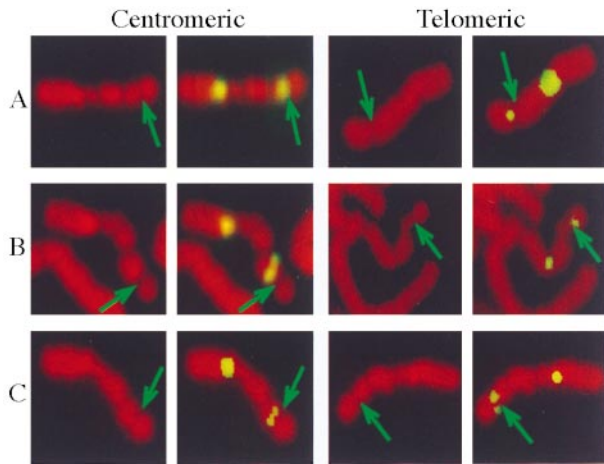
FIG. 2. Examples of hybridization signals centromeric and telomeric to *FRA7H*. FISH analysis was performed on metaphase chromosomes expressing *FRA7H* from two cell lines: GM00847 (*A* and *C*) and GM10791A (*B*). FISH experiments were performed with fluorescein isothiocyanate (FITC)-labeled YAC HSC7E186 (*A* and *B*) or cosmid 141e11 (*C*) cohybridized with a probe for chromosome 7 centromere. Propidium staining (left panel in each pair) and FISH with FITC-labeled probes (right panel in each pair) are shown. Arrows point to *FRA7H*.

exclude the possibility, however, that *FRA7H* constitutes a large gene, as reported for *FRA3B* (33).

Helix Flexibility and Stability. In the absence of any obvious DNA sequences that could account for the fragility we undertook a new approach. The *FRA7H* sequence was analyzed for structural characteristics of the DNA sequence that might be associated with the fragility. In rare fragile sites the expanded CGG repeats affect helix flexibility, leading to repression of nucleosome assembly, decondensation, and fragility (34, 35). Accordingly, we first searched the *FRA7H* sequence for potential local variations in the DNA flexibility, which appears to play an important role in protein–DNA interactions and hence might affect chromatin condensation (25). The analysis revealed four regions with potential high flexibility deviating significantly (>4.5 SD, based on the value of the lowest region among the four) from the average value of the entire *FRA7H* sequence ($\bar{x}$ = 10.7°; SD =

Table 2. FISH analysis of cosmids hybridization signals on chromosomes expressing *FRA7H*

Cosmid clone	Color	No. of signals		
		Centromeric	On	Telomeric
210c9	Orange	—	—	11
141e11	Purple	5	3	4
108f11/92h2	Dark green	23	1	2
72c11	Gray	6	3	2
137g12	Pink	9	4	7
159c12	Blue	4	—	5
35c9	Brown	3	2	3
62f7	Light green	10	—	—

Analysis of hybridization signals on metaphase chromosomes expressing *FRA7H* from cell line GM00847. The clones are ordered in accordance with the physical map, centromeric (top of the table) to telomeric (bottom). The results of clones covering the same genomic region were combined. The colors mark cosmid clones in Fig. 3.

0.65; $P < 0.0001$) (Fig. 4*A*). Three of these regions are clustered within a 33-kb region (Fig. 4*A*). The SV40 and the *ZNF131* integration sites are located only 1–2 kb from high-flexibility regions (Fig. 5).

To assess the significance of the potential high-flexibility pattern identified in the *FRA7H* region, we analyzed 1.1 Mb composed of 14 genomic sequences mapped to chromosomal bands in which fragile sites were not described (GenBank locus names: hsablgr1, hsablgr2, hsl185e6a, hsl19h1, hsl247f6, hsl79f5a, hsq25, hsq27, hsu07000, hsu09822, hsu29953, hsu36341, hsu40455, hsu41384, humhprtb, hsu52111, hsu52112, and humretblas). The analysis revealed that regions with high flexibility appear every ≈100 kb (Fig. 4*B*). Thus, regions with high flexibility in *FRA7H* are more frequent than predicted by the control analysis.

We also analyzed the *FRA7H* sequence for helix stability. The analysis revealed seven sites with potential low stability that deviated significantly (>2.5 SD) from the average value of the entire *FRA7H* sequence ($\bar{x}$ = 1.57 kcal/mol, SD = 0.124, $P < 0.0062$), based on the value for highest region among the

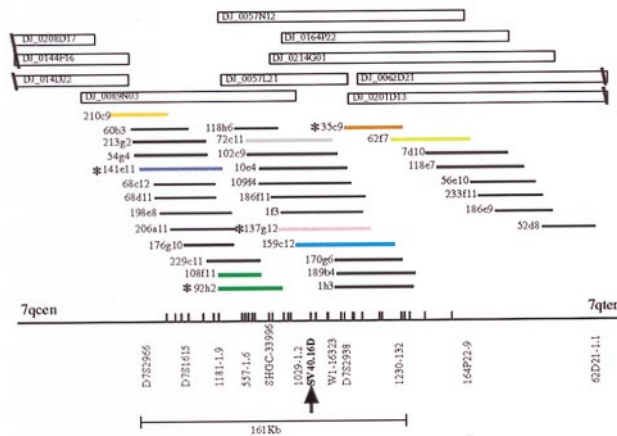FIG. 3. A cosmid and PAC map covering the *FRA7H* region. P1-derived artificial chromosome (PAC) clones (name DJ_plate_row_column) and cosmids clones covering the region between markers *D7S786* and *62D21–1.1* (see Fig. 1 for position within 7q32) are shown. Vertical bars along the horizontal baseline represent *Eco*RI sites. The region representing the 161-kb sequence contig is shown below. Asterisks indicate cosmids that were sequenced. Cosmids that were used for the FISH analysis are marked by colors. Clones covering the same region are marked by the same color.
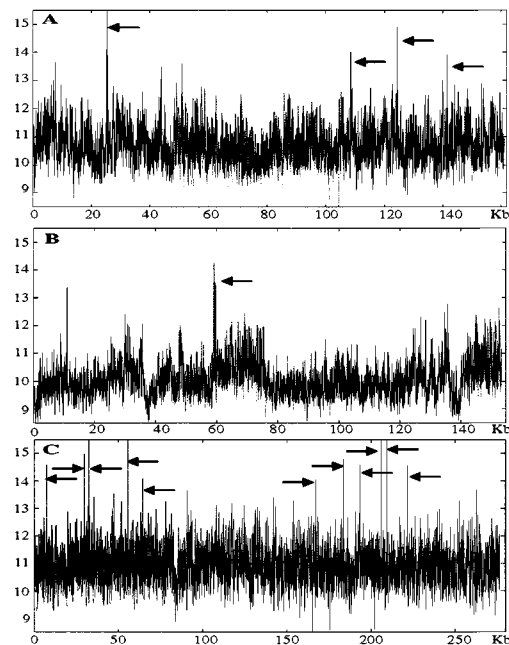

FIG. 4. Analysis of DNA flexibility. Arrows point to regions with significantly high flexibility. *x* axis, nucleotide position at the beginning of a 100-bp window. *y* axis, degrees of inclination in the twist angel. (*A*) *FRA7H* region. (*B*) Example of a control sequence, hsu52111. (*C*) *FRA3B* combined sequences.
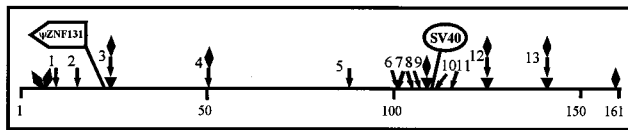
FIG. 5. Map of *FRA7H* showing DNA regions of high flexibility (▼), low stability (♦), and non-B-DNA structure (↓). The SV40 integration site and the *ZNF131* pseudogene are marked. The numbers below the map represent the base location in *FRA7H*.

seven sites. All the regions in *FRA7H* that were predicted to show high flexibility also showed low stability (Fig. 5).

Potential Non-B-DNA Sequences. The replication of rare fragile sites with CGG expansion is delayed relative to that of normal alleles (36, 37). CGG repeats have a propensity to adopt a non-B-DNA structure (hairpin or tetraplex), leading to arrest of DNA replication *in vitro* (38–40) and *in vivo* (41). The replication of the common fragile site *FRA3B* is delayed by exposing cells to the fragile site inducer aphidicolin (42). Hence, we searched the *FRA7H* region for two types of potential non-B-DNA sequences under negative superhelical strain: triple helixes and MARs. Triple-helix-forming sequences play an important role in triggering gene expression and homologous recombination (43), block DNA replication *in vitro* (44), and decrease the efficiency of replication *in vivo* (45). The MARs are prone to unwinding by continuous base unpairing (46). Chromosomal attachments to the nuclear matrix create independent loop domains that affect DNA replication, transcription, and condensation (47). Our analysis revealed 13 sites with non-B-DNA-forming potential, 6 sites with potential to form a triple-helical DNA structure (sites 1, 2, 4, 7, 8, and 10), and 7 potential MARs (sites 3, 5, 6, 9, 11, 12, and 13; Fig. 5). Six of these (sites 6–11) were in a cluster that colocalized with a high flexibility and low stability and with the SV40 integration site (Fig. 5). Thus, the frequency and distribution of these sites might be an important feature of the *FRA7H* region.

In Vitro Analysis of Non-B-DNA Structures. CAA has been used for non-B-DNA structure analysis (48). CAA reaction is ideal for detecting only unpaired bases (even only a single unpaired base) within double-stranded DNA (29). *In vitro* analysis of triple-helix formation was performed on a 4.4-kb *Eco*RI fragment, cloned from cosmid 137g12 (base position 106,853–111,288) (Fig. 4), which harbors the SV40 integration site and a potential triple helix site with a 39 homopyrimidine tract (site 10, Figs. 5 and 6). When a homopyrimidine/homopurine sequence forms triple helix structure (Py·Pu·Py
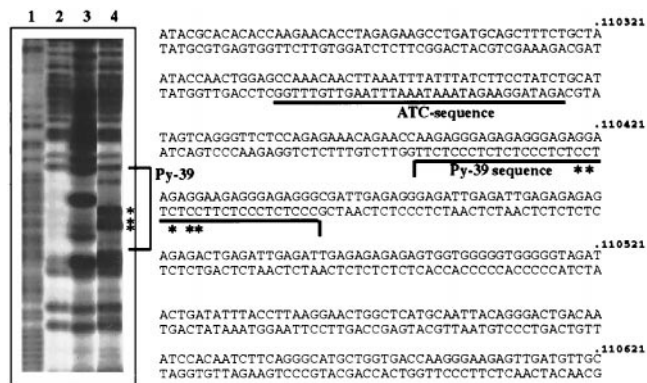

FIG. 6. Non-B-DNA structure adopted by plasmid DNA containing site 10. Plasmid DNA with the 4.4-kb *Eco*RI fragment was unmodified (lanes 1 and 2) or modified with CAA (lanes 3 and 4). Lane 1, hydrazine reaction of control DNA. Lanes 2–4, formic acid reaction of control DNA (lane 2), CAA-treated DNA in the absence of Mg^{2+}, at pH 7 (lane 3), and CAA-treated DNA in the presence of Mg^{2+}, at pH 7 (lane 4). The nucleotide sequence is from *FRA7H* sequence. The asterisks mark sites that reacted prominently with CAA.

triplex, H-DNA) the center of the homopyrimidine strand and the purine bases over the 5′ half of the homopurine strand are unpaired and are reactive with CAA. Thus, the H-DNA structure can be demonstrated by the cleavage of DNA at these CAA-modified residues. CAA-reacted cytosines were detected in the center of the Py-39 of site 10 in the presence of Mg^{2+} at pH 7, conditions that support the formation of H-DNA (Fig. 6, lane 4). Under the same conditions, CAA-reacted adenines were also detected over the 5′ half of the purine strand of the Py-39 sequence (data not shown). Thus, the predicted site of potential non-B-DNA structure was proved to form non-B-DNA structure under torsional stress *in vitro*. In the absence of metal ions the Py-39 sequence also showed a strong unpaired DNA structure (Fig. 6, lane 3 compared with the control lane 2) with a CAA-reactive pattern different from that of a normal H-DNA structure (Fig. 6, lane 4). The nature of this pattern is unknown, and it might be affected by the nearby ATC sequence (Fig. 6). *In vitro* analysis of an adjacent 2.2-kb *Eco*RI fragment (position 104,637–106,853), in which no sites were predicted, did not reveal any apparent non-B-DNA sequences (data not shown). Further studies are required to investigate the *in vivo* role of such unusual DNA structures in the fragility mechanism.

***FRA7H* Shows Unusual Chromatin Organization.** Our extensive FISH studies identified nonoverlapping cosmid clones that showed FISH signals spanning *FRA7H* (Fig. 3, Table 2). These results suggest that the under-condensation of induced fragile sites can occur at different locations along the fragile region. Similar FISH patterns have been seen for other fragile sites.

Several YAC and cosmid clones, flanking the 161-kb sequenced region, showed FISH signals in opposite orientation relative to the physical map (Figs. 1 and 3, Tables 1 and 2). Similarly, clones spanning *FRA3B* yielded signals in opposite orientation on chromosomes from different individuals (13, 15, 17). We cannot exclude the possibility that genomic rearrangements associated with the region surrounding the fragile site might account for these FISH observations. We speculate, however, that the unexpected nonlinear FISH hybridization patterns at fragile sites might reflect regions of chromatin organization in which the linearity of the DNA relative to the chromosomal axis is altered.

Comparison of *FRA7H*, *FRA3B*, and the Putative Partial Sequence of *FRA7G*. To identify shared sequence features between aphidicolin-induced common fragile sites, we first compared the sequences of *FRA7H* and *FRA3B* (GenBank accession no. AF017104 and U66722, respectively). Both regions are A+T-rich (58% and 61%, respectively) and are gene poor. In both fragile sites insertions of viral genomes and pseudogenes occurred, further indicating that fragile sites are unstable regions.

To assess the relevance of the high-flexibility and low-stability patterns to the aphidicolin-induced fragility, we analyzed the *FRA3B* combined sequences (GenBank accession nos. U66722 and AF020503). Eleven regions with potential high flexibility were identified, with values comparable to those of the high regions of *FRA7H*. These regions appeared in two clusters (Fig. 4*C*). One of the regions with high flexibility is at the same site as a reported aphidicolin-induced breakpoint cluster (position 39,597, GenBank accession no. U66722, position 205,959 in Fig. 4*C*). Interestingly, this site meets many of the criteria for being a MAR (49). We also analyzed the stability pattern of *FRA3B* and revealed that the high-flexibility and low-stability regions colocalized, as in the *FRA7H* region (data not shown). The impressive cluster of high-flexibility and low-stability regions in *FRA3B* might reflect the fact that it is the most inducible common fragile site in the human genome. Thus, regions with high flexibility and low stability, in *FRA7H* and *FRA3B*, might contribute to the overall chromatin structure of these fragile sites and hence to their breakage and rearrangement.

We also searched for similarity in the repeat free sequences between *FRA7H* and *FRA3B*. The comparison revealed similarities (>95%) among short sequences within the regions with high flexibility. These sequences are A+T-rich, as expected from the flexibility value for this dinucleotide (25). Thus, these short sequence elements might be associated with the fragility of both *FRA7H* and *FRA3B*. Sequence similarities (>95%) were also found in two of the regions predicted to form non-B-DNA structure in *FRA7H* (sites 3 and 7). Together these observations indicate that *FRA7H* and *FRA3B* share sequence similarities in regions with potential to form unusual DNA structure, and they support our contention that the unusual DNA structure may be associated with the mechanism of fragility in *FRA7H* and *FRA3B*. Nine additional sequences of 17–22 bp showed sequence similarity of >95% between the two fragile sites, the significance of which needs further investigation.

It was of interest to analyze the *FRA7G* sequence; however, the region spanned by *FRA7G* is not completely defined. Nevertheless, we performed analysis of helix flexibility and stability on the available 150-kb sequence harboring the DNA marker *D7S522* reported to be part of *FRA7G* (accession. no. AC002066; ref. 18). Eight regions with potential high flexibility were identified. Three of these sites were clustered within 18 kb harboring *D7S522* (data not shown). Similarly to *FRA7H* and *FRA3B*, the stability pattern of *FRA7G* revealed that the high-flexibility and low-stability regions colocalized (data not shown).

We also searched for similarity in the repeat free sequences between *FRA7H* and the partial sequence of *FRA7G*. The comparison revealed similarities (>95%) among short sequences, the significance of which needs further investigation.

In summary, we identified a common fragile site, *FRA7H*, by cloning a viral integration site. This approach could be of general value for the isolation of common fragile sites in the human genome. Sequence analysis of *FRA7H* and *FRA3B* revealed several sequence-based features that are suggestive of unusual DNA structures. The sequence analysis of the putative partial *FRA7G* also revealed similar features. These are possibly intrinsic properties of common fragile sites that may affect their replication and condensation as well as organization and may lead to fragility. Identification and characterization of other aphidicolin-induced common fragile sites and studies of specific regions within these sites are required to understand the significance of the unusual DNA structures found in *FRA7H*, *FRA3B,* and *FRA7G* for the general mechanism of fragility.

1. Sutherland, G. R. & Richards, R. I. (1995) *Curr. Opin. Genet. Dev.* **5,** 323–327.
2. Oberle, I., Rousseau, F., Heitz, D., Kretz, C., Devys, D., Hanauer, A., Boue, J., Bertheas, M. F. & Mandel, J. L. (1991) *Science* **252,** 1097–1102.
3. Gecz, J., Gedeon, A. K., Sutherland, G. R. & Mulley, J. C. (1996) *Nat. Genet.* **13,** 105–108.
4. Jones, C., Penny, L., Mattina, T., Yu, S., Baker, E., Voullaire, L., Langdon, W., Sutherland, G., Richards, R. & Tunnacliffe, A. (1995) *Nature (London)* **376,** 145–149.
5. Kremer, E. J., Pritchard, M., Lynch, M., Yu, S., Holman, K., Baker, E., Warren, S. T., Schlessinger, D., Sutherland, G. R. & Richards, R. I. (1991) *Science* **252,** 1711–1714.
6. Knight, S., J., Flannery, A. V., Hirst, M. C., Campbell, L., Christodoulou, Z., Phelps, S. R., Pointon, J., Middleton-Price, H. R., Barnicoat, A., Pembrey, M. E., *et al.* (1993) *Cell* **74,** 127–134.
7. Nancarrow, J., Kremer, E., Holman, K., Eyre, H., Doggett, N., Le Paslier, D., Callen, D., Sutherland, G. & Richards, R. (1994) *Science* **264,** 1938–1941.
8. Parrish, J. E., Oostra, B. A., Verkerk, A. J., Richards, C. S., Reynolds, J., Spikes, A. S., Shaffer, L. G. & Nelson, D. L. (1994) *Nat. Genet.* **8,** 229–235.
9. Yu, S., Mangelsdorf, M., Hewett, D., Hobson, L., Baker, E., Eyre, H. J., Lapsys, N., Le Paslier, D., Doggett, N. A., Sutherland, G. R. & Richards, R. I. (1997) *Cell* **88,** 367–374.
10. Kornberg, A. & Baker, T. A. (1992) *DNA Replication* (Freeman, New York).
11. Wilke, C. M., Guo, S. W., Hall, B. K., Boldog, F., Gemmill, R. M., Chandrasekharappa, S. C., Barcroft, C. L., Drabkin, H. A. & Glover, T. W. (1994) *Genomics* **22,** 319–326.
12. Paradee, W., Wilke, C. M., Wang, L., Shridhar, R., Mullins, C. M., Hoge, A., Glover, T. W. & Smith, D. I. (1996) *Genomics* **35,** 87–93.
13. Wilke, C. M., Hall, B. K., Hoge, A., Paradee, W., Smith, D. L. & Glover, T. W. (1996) *Hum. Mol. Genet.* **5,** 187–195.
14. Boldog, F., Gemmill, R. M., West, J., Robinson, M., Robinson, L., Li, E., Roche, J., Todd, S., Waggoner, B., Lundstrom, R., Jacobson, J., Mullo-kandov, M. R., Klinger, H. & Drabkin, H. A. (1997) *Hum. Mol. Genet.* **6,** 193–203.
15. Zimonjic, D. B., Druck, T., Ohta, M., Kastury, K., Croce, C. M., Popescu, N. C. & Huebner, K. (1997) *Cancer Res.* **57,** 1166–1170.
16. Inoue, H., Ishii, H., Alder, H., Snyder, E., Druck, T., Huebner, K. & Croce, C. M. (1997) *Proc. Natl. Acad. Sci. USA* **94,** 14584–14589.
17. Rassool, F. V., Le Beau, M. M., Shen, M.-L., Neilly, M, E., Espinosa, R., III, Ong, S. T., Boldog, F., Drabkin, H., McCarroll, R. & McKeithan, T. W. (1996) *Genomics* **35,** 109–117.
18. Huang, H., Qian, C., Jenkins, R. B. & Smith, D. I. (1998) *Genes Chromosomes Cancer* **21,** 152–159.
19. Popescu, N., Zimonjic, D. & DiPaolo, J. (1990) *Hum. Genet.* **84,** 383–386.
20. Smith, P. P., Friedman, C. L., Bryant, E. M. & McDougall, J. K. (1992) *Genes Chromosomes Cancer* **5,** 150–157.
21. Scherer, S. W., Tompkins, B. J. & Tsui, L. C. (1992) *Mamm. Genome* **3,** 179–181.
22. Ioannou, P. A., Amemiya, C., Garnes, J., Kroisel, P. M., Shizuya, H., Batzer, M. A. & de Jong, P. J. (1994) *Nat. Genet.* **6,** 84–88.
23. Lichter, P., Cremer, T., Borden, J., Manuelidis, L. & Ward, D. C. (1988) *Hum. Genet.* **80,** 224–234.
24. Craxton, M. (1993) *Methods Mol. Biol.* **23,** 149–167.
25. Sarai, A., Mazur, J., Nussinov, R. & Jernigan, R. L. (1989) *Biochemistry* **28,** 7842–7849.
26. Breslauer, K. J., Frank, R., Blocker, H. & Marky, L. A. (1986) *Proc. Natl. Acad. Sci. USA* **83,** 3746–3750.
27. Frank-Kamenetskii, M. D. & Mirkin, S. M. (1995) *Annu. Rev. Biochem.* **64,** 65–95.
28. Dickinson, L. A., Joh, T., Kohwi, Y. & Kohwi-Shigematsu, T. (1992) *Cell* **70,** 631–645.
29. Kohwi, Y. & Kohwi-Shigematsu, T. (1988) *Proc. Natl. Acad. Sci. USA* **85,** 3781–3785.
30. Mitchell, A. R., Ambros, P., Gosden, J. R., Morten, J. E. & Porteous, D. J. (1986) *Somat. Cell Mol. Genet.* **12,** 313–324.
31. Campo, M. S., Cameron, I. R. & Rogers, M. E. (1978) *Cell* **15,** 1411–1426.
32. Kunz, J., Scherer, S. W., Klawitz, I., Soder, S., Du, Y. Z., Speich, N., Kalff-Suske, M., Heng, H. H., Tsui, L. C. & Grzeschik, K. H. (1994) *Genomics* **22,** 439–448.
33. Ohta, M., Inoue, H., Cotticelli, M. G., Kastury, K., Baffa, R., Palazzo, J., Siprashvili, Z., Mori, M., McCue, P., Druck, T., *et al.* (1996) *Cell* **84,** 587–597.
34. Metzenberg, S. (1996) *Am. J. Hum. Genet.* **59,** 252–253.
35. Wang, Y.-H., Gellibolian, R., Shimizu, M., Wells, R. D. & Griffith, J. (1996) *J. Mol. Biol.* **263,** 511–516.
36. Hansen, R. S., Canfield, T. K., Lamb, M. M., Gartler, S. M. & Laird, C. D. (1993) *Cell* **73,** 1403–1409.
37. Subramanian, P. S., Nelson, D. L. & Chinault, A. C. (1996) *Am. J. Hum. Genet.* **59,** 407–416.
38. Fry, M. & Loeb, L. A. (1994) *Proc. Natl. Acad. Sci. USA* **91,** 4950–4954.
39. Usdin, K. & Woodford, K. J. (1995) *Nucleic Acids Res.* **23,** 4202–4209.
40. Weitzmann, M. N., Woodford, K. J. & Usdin, K. (1997) *J. Biol. Chem.* **272,** 9517–9523.
41. Samadashwily, G. M., Raca, R. & Mirkin, S. M. (1997) *Nat. Genet.* **17,** 298–304.
42. Le Beau, M. M., Rassool, F. V., Neilly, M. E., Espinosa, R., III, Glover, T. W., Smith, D. I. & McKeithan, T. W. (1998) *Hum. Mol. Genet.* **7,** 755–761.
43. Kohwi, Y. & Kohwi-Shigematsu, T. (1991) *Genes Dev.* **5,** 2547–2554.
44. Baran, N., Lapidot, A. & Manor, H. (1991) *Proc. Natl. Acad. Sci. USA* **88,** 507–511.
45. Rao, B. S., Manor, H. & Martin, R. G. (1988) *Nucleic Acids Res.* **16,** 8077–8094.
46. Kohwi-Shigematsu, T. & Kohwi, Y. (1990) *Biochemistry* **29,** 9551–9560.
47. Bode, J., Kohwi, Y., Dickinson, L., Joh, T., Klehr, D., Mielke, C. & Kohwi-Shigematsu, T. (1992) *Science* **255,** 195–197.
48. Kohwi-Shigematsu, T. & Kohwi, Y. (1992) *Methods Enzymol.* **212,** 155–180.
49. Wang, L., Paradee, W., Mullins, C., Shridhar, R., Rosati, R., Wilke, C. M., Glover, T. W. & Smith, D. I. (1997) *Genomics* **41,** 485–488.